Reductive/expansion synthesis of zero valent submicron and nanometal particles

Hugo Zea
Departamento de Ingeniería Química y Ambiental, Universidad Nacional de Colombia, Bogota, Colombia

Claudia C. Luhrs
University of New Mexico, Department of Mechanical Engineering, Albuquerque, New Mexico 87131

Jonathan Phillips[a)]
University of New Mexico, Department of Mechanical Engineering, Albuquerque, New Mexico 87131; and Los Alamos National Laboratory, Los Alamos, New Mexico 87544

(Received 2 August 2010; accepted 12 October 2010)

Upon rapid heating to a high temperature (~800 °C), mixtures of nitrate compounds and urea created nano and submicron metal particles. The process (reductive/expansion synthesis, RES) results in atomic scale mixing. The product formed from mixed-nitrate (Fe + Ni) salts and urea created true metallic alloy. Unlike other product-from-powder synthesis processes, this process produced only zero valent metal. Initial work suggests this method is a scalable and efficient means for making metallic nanoparticles. Although this is primarily a phenomenological report, a preliminary model is presented: Initially, nitrates decompose to oxide; thus in the absence of urea metal oxide particles form, as in the case of combustion synthesis. In the case of urea/nitrate mixtures, there is a "convolution" of decomposition processes. Urea decomposes to yield reducing gases, leading to the formation of metal rather than oxide. Rapid "expansion" of gas leads to "shattering," resulting in highly dispersed particles.

I. INTRODUCTION

Many applications have been proposed for nanoparticles: armor, surface coating, data storage, inks, bioimaging applications,[1–3] sinter-resistant plasma-generated catalysts.[4–7] The recent demonstration that complex nanoparticles, that is nanoparticles with multiple shells,[8,9] and/or designed void spaces,[10] suggests other applications such as anode or cathode materials for high-energy density batteries, and light, high energy density solid fuels. Enabling these technologies will require means to make large quantities of nanoparticles. There are many processes for making primarily metallic nanoparticles including several aerosol techniques: aerosol-through-plasma (A-T-P),[4–13] evaporation of solvents from small drops containing dissolved salts[14,15] and flame synthesis.[16–18] Nonaerosol processes for making nanometal particles include metal gas evaporation,[19] metal evaporation in a flowing gas stream,[20] mechanical attrition,[21] sputtering,[22] electron beam evaporation,[23] electron beam induced atomization of binary metal azides,[24] expansion of metal vapor in a supersonic free jet,[25] inverse micelle techniques,[26] laser ablation,[27] laser-induced breakdown of organometallic compounds,[28] and pyrolysis of organometallic compounds.[29]

The present technique, reductive/expansion synthesis (RES), is not closely related to any of the aforementioned in terms of either process or mechanism. The process, clearly unique, requires only two steps: (i) molecular, partially oxidized metal precursors (e.g., iron nitrate) are physically combined with a chemical reducing agent (i.e., urea) that releases gaseous reducing species upon reaching its decomposition temperature, and (ii) the mixture is heated until the reducing agent decomposes, at which point the process is terminated. The postulated mechanism is also unique. All data are consistent with a "three-step mechanism;" however, it must be noted that the steps are convoluted, rather than readily separated. First, the metal precursor decomposes to create submicron scale metal oxide. (This is very similar to the single-step process known as combustion synthesis.) The "next" step, although convoluted with the first, is that the reducing agent (e.g., urea) decomposes to release "reducing" gases. Third, the gases produced from the convoluted decomposition steps physically "disperse" the metal particles.

To demonstrate the RES method, several different metal products were targeted and the results successful in each case. Batches of single-metal submicron and nanoscale particles of single metal (Ni, Fe) and alloy (Fe–Ni) were produced by rapidly heating mixtures of appropriate nitrates and urea. Recovered product consisted entirely of "submicron" and nanometallic particles, often agglomerated into micron scale. Other data support the

[a)]Address all correspondence to this author.
e-mail: jcbc@cableone.net
DOI: 10.1557/jmr.2010.66

 © Materials Research Society 2011

https://doi.org/10.1557/jmr.2010.66 Published online by Cambridge University Press

mechanistic hypothesis. In particular in the absence of urea, large (~10 μm) metal oxide particles composed of aggregated submicron and nanometal oxide particles were produced from nitrates. This is consistent with the mechanistic postulate that reduced metal particles are formed from the reduction of oxide precursor particles. One caveat of the initial work: Carbon was present in the particles, either forming a thin graphite layer (Ni and Fe–Ni) or some carbide (Fe).

II. EXPERIMENTAL

A. Generation

The RES synthesis process used herein involves only two major steps: physical mixing metal precursor nitrate salt with urea and rapid heating of the mixture under inert atmosphere. The time period for heating, about 180 s, was chosen to ensure the complex decomposition process of urea and nitrates (initially at ambient temperature), is complete (~500 °C).

The mixtures used (see Table I for particular sample compositions) contained urea (Aldrich 99.9%), $Fe(NO_3)_3{\cdot}9H_2O$ (iron nitrate nonahydrate, Aldrich 99.9%) and/or $Ni(NO_3)_2{\cdot}6H_2O$ (nickel nitrate hexahydrate, Aldrich, 99.99%). For example, to make Fe–Ni alloy (1:1 atomic stoichiometry) nanoparticles 0.25 g of $Fe(NO_3)_3{\cdot}9H_2O$, 0.1825 g of $Ni(NO_3)_2{\cdot}6H_2O$ and 2 g of urea were added to an alumina mortar and ground until a green paste, homogenous in appearance, formed. The paste was transferred to an alumina boat (4 × 1 × 1 cm) and "kneaded" gently with a small spatula to remove any gross scale air pockets. The boat was then maneuvered to the center of a quartz tube (2.5 cm outside diameter × 30 cm length), through which nitrogen (99.999%) was passed (400 mL/m) for at least 20 min (to remove air). The second "step" is simply to quickly open a preheated (800 °C) clamshell furnace, place the preloaded quartz tube inside, with gas mixture still flowing, and then close the furnace.

Notably, approximately 90 s after the tube is placed in the furnace, a white smoke fills the tube downstream from the precursor boat. This delay represents the time for the urea in the mix to reach its full decomposition temperature, approximately 500 °C. (No "smoke" was observed in the absence of urea.) The smoke stops evolving in just a few seconds, although a white film on the section of tube extending beyond the edge of the oven remains.

TABLE I. Metal–metal and metal(s)–urea ratios for the preoven mixtures.

	Sample	Fe/Ni atomic ratio	Fe–Ni salts/urea weight ratio
1	Ni	0/1	1/4.5
2	Fe	1/0	1/4.5
3	Fe–Ni	1/1	1/4.5
4		1/1	1/0

The process used is a simple means to ensure rapid heating and reasonable batch product volumes, but is not conducive to perfect temperature control. Indeed, opening the clamshell furnace and placing the quartz reactor led to a decrease in the nominal furnace temperature to 650 ± 25 °C. The furnace does reheat upon closure, generally just reaching a nominal 800 °C during the ~180 s heating process.

Approximately 180 s after the reactor is placed in the furnace, the clamshell furnace is reopened and the reactor removed and placed in an ambient temperature cradle, while gas continues to flow. The final step is recovery of the product from the boat once the sample is thoroughly cooled (~25 min). In addition, the white powder scrapped from the end section of the quartz tube outside the oven was removed for independent examination.

B. Characterization

A scanning electron microscope (SEM; Hitachi S5200 nano) and a transmission electron microscope (TEM; JEOL 2010), equipped with energy-dispersive spectroscopy (EDS), were used. For both SEM and TEM, samples were prepared "dry." That is, the powders were removed from the alumina boat in which they were created and placed directly on sample holders. An x-ray diffractometer (XRD), Scintag Pad V diffractometer/goniometer with Scintillation detector and Datascan software was used for the XRD studies. All instruments are located at the University of New Mexico.

Thermogravimetric analysis (TGA; Netzsch STA409 PC Luxx) was used to study the "decomposition" process of three mixtures: "neat" nickel nitrate, neat urea, and nickel nitrate + urea. In all cases, approximately 20 mg of material (mixed according to the ratios given in Table I) were placed in the sample cup of the instrument, nitrogen gas (99.99% Air Products) flowed through the instrument and temperature ramped at a steady rate from ambient to 800 °C.

III. RESULTS

A. Fe–Ni (Sample 1, Table I)

Examination of particles generated from a mixture (1Fe:1Ni) of iron and nickel nitrate clearly shows that metal was generated with an average particle size of about 100 nm. As shown in the SEM pictures [Figs. 1(a), 1(b)], particle sizes ranged from 50 to about 250 nm. The TEM observations of the sample [Fig. 1(c)] show particles in the same size range. A particle size distribution based on the SEM results is shown in Fig. 2. The pictures suggest that many of the particles most removed from spherical shape are actually "agglomerates" of smaller particles, such that the average "primary particles" may be smaller than the average suggested by Fig. 2.

https://doi.org/10.1557/jmr.2010.66 Published online by Cambridge University Press

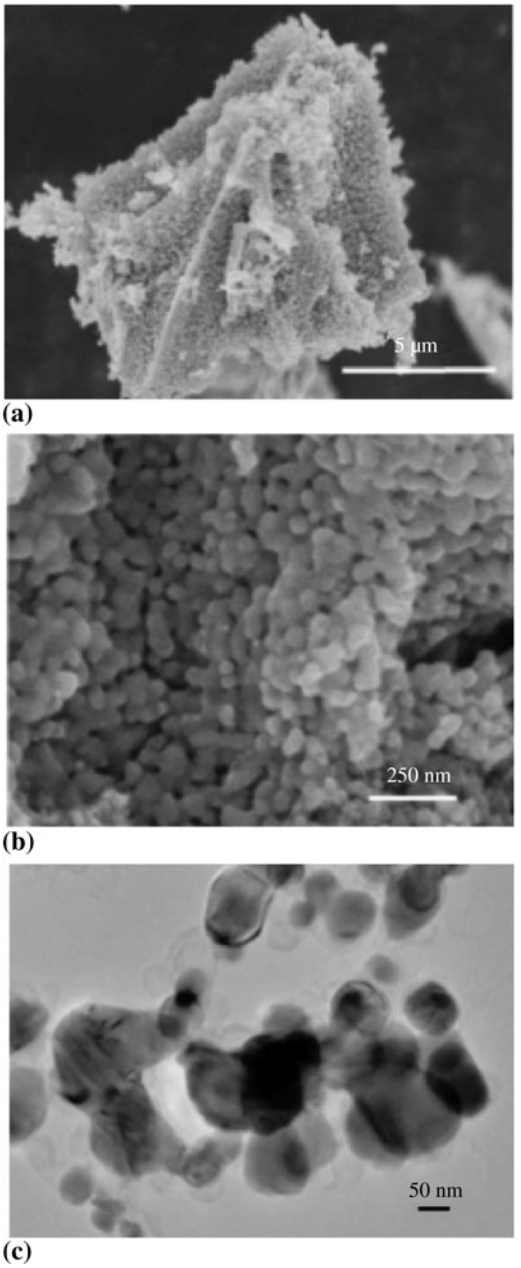


FIG. 1. Electron microscopy of alloy particles. (a) and (b) SEM shows micron-scale agglomerates composed of "primary" Fe–Ni particles between 50 and 150 nm in size. (c) TEM studies confirm the "primary" alloy particles are of the order 150 nm in size.

TEM results support the supposition that many/most of the high aspect ratio particles seen in SEM are agglomerates of a small number of primary, nearly spherical, particles. No primary particles greater than 150 nm in maximum dimension were found. The particle sizes observed using TEM, on a very small sample size, are consistent with expectations based on the SEM analysis. TEM analysis also revealed that a thin shell, always less than 10 nm, of graphitic carbon was found on all the metal particles examined (Fig. 3).

The structure and semiquantitative composition of the particles are clear from both XRD (Fig. 4, top) and EDS analysis: true, metallic, Fe–Ni alloys with a graphitic coating. The FeNi peaks are clearly visible, as marked in Fig. 4. A small peak, probably graphite, is found at ~26° 2θ. As a control, a similar experiment was conducted with pure argon, in place of the Ar/H_2 mix. In that case, a small oxide peak (8% the intensity of Fe + Ni peaks) was observed.

B. Fe only

Using iron nitrate/urea mixtures (Table I, Sample 2), XRD data shows that both metallic iron and iron carbide are present. Both the XRD data (Fig. 4) and EDS analysis of the fiberlike particles (Fig. 5) suggest that some of the particles are actually iron carbide. The particles are similar in size to FeNi and Ni only cases.

C. Ni only

It is informative to contrast the particles formed from nickel nitrate with and without urea. From XRD analysis, it is clear that metallic particles (no carbide) are produced [Fig. 4(c)] from a mixture of urea and nickel nitrate, whereas only NiO is formed using an identical protocol, but starting with "neat" nickel nitrate as the precursor [Fig. 4(d)]. The latter result is consistent with the results of earlier studies of the thermal decomposition of nitrates[30] particularly nickel nitrate.[31] The absence of nickel carbide is consistent with the fact that nickel carbide decomposes above ~300 °C.[32]

The SEM provides a very interesting contrast. At a large scale (~500 μm) the "texture" of the two samples, after gentle "spreading" with a small spatula, is very different [Figs. 6(a) and 6(b)]. The sample prepared with urea appears as a uniform layer of "very fine" powder at this scale, whereas the sample prepared without urea clearly consists of particles with an average size of more than 10 μm. This difference is not maintained at finer scale. Indeed, the bottom panels of Fig. 6 show that both samples are composed, apparently entirely, of "primary" particles of nearly the same size. That is, the large NiO particles appear to be aggregates of particles of the order 100 nm in size. The "fine powder" of the metallic nickel is also composed of particles of the same order of size, but more loosely bound (agglomerates).

It is also interesting to note some qualitative differences with regard to agglomeration/aggregation. The metal particle sample is easily spread with a small spatula (0.5 cm blade) to form uniform films on all scales, whereas the same protocol with the metal oxide particles leaves "broken" particles (see Fig. 6), but clearly not smooth films. (Prior to "spreading" with a small spatula, the Ni-only metal particles were in agglomerates similar to those found in Fig. 1). The qualitative evidence supports

https://doi.org/10.1557/jmr.2010.66 Published online by Cambridge University Press

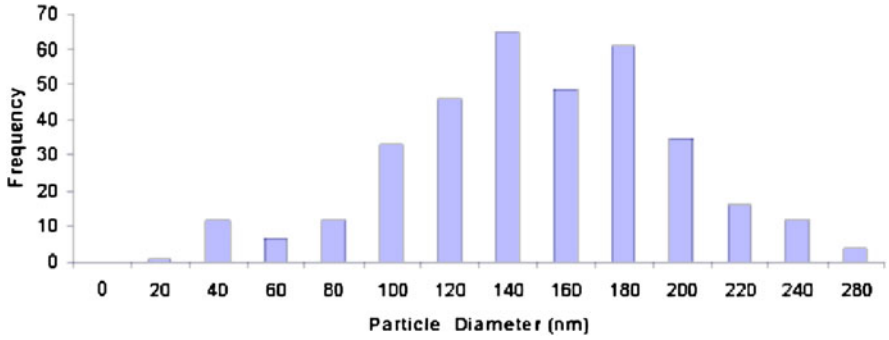


FIG. 2. Fe–Ni (urea) sample particle size distribution. Based on measurements of maximum dimension, the mean particle size is about 150 nm.

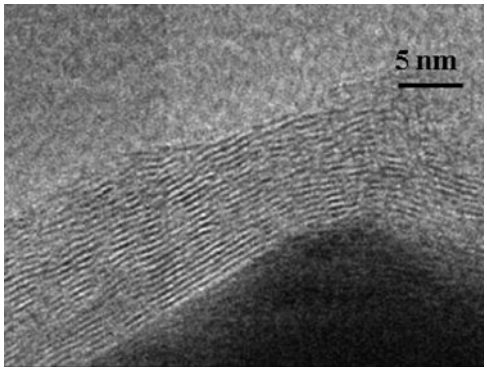


FIG. 3. Graphitic shell. A thin carbon (graphitic) layer was found on the alloy particles.

the postulate that the metal particles form (weakly bound) agglomerates, possibly a result of the graphite coatings. In contrast, the oxides particles are apparently true aggregates. Quantification of agglomeration/aggregation[33] was not performed for this first study.

D. Thermogravimetric analysis

Three samples were studied under the same conditions of gas flow and temperature ramp rate: (a) Ni $(NO_3)_2{\cdot}6H_2O$, (b) urea, and (c) the mixture 1:4.5 in wt. of metal salt and urea.

The TGA of the nickel nitrate decomposition was very similar to that reported elsewhere.[32] Urea decomposed in two well-distinguished stages: first step in the range of 220 to 250 °C, and then a second step between 360 and 380 °C.[34] The first stage is believed to correspond to urea decomposition to form ammonia and isocyanic acid:

$$(NH_2)_2CO \rightarrow NH_3 + HNCO \quad .$$

The second stage will primarily render ammonia and carbon dioxide:

$$HNCO + H_2O \rightarrow NH_3 + CO_2 \quad .$$

Earlier studies indicate the decomposition of urea is very dependent on mixture chemistry. For example, it is reported that in the presence of water cyanic acid, cyanuric acid, burret, and higher molecular weight products during decomposition.[35] Thus, the decomposition of a typical reactive mix was studied. As expected, the outcome was not simply the sum of nitrate and urea decomposition.

The TGA analysis of Ni nitrate hexahydrate plus urea shows the thermal decomposition of the mixture takes place in four stages. It is clear that the two processes are convoluted; thus it is impossible to list a clear "order" to the decomposition process. The first step (A) appears to relate to both nitrate and urea decomposition processes. The nitrate loses all structural water by 250 °C. This result is consistent with the generally accepted model of hydrated nitrates: Water molecules attached to their structure are lost without disrupting the nitrate groups. In addition, urea decomposition is well underway during step A and based on the process of pure urea decomposition it is expected ammonia and isocyanic acid are produced. The second step (B, ~250 to 300 °C) corresponds solely to a nitrate decomposition process: loss of all the NOx groups, leaving NiO as solid by-product at temperatures close to 350 °C. Steps C (~300–360 °C) and D (~360–500 °C) are clearly a reflection of some chemical interaction between nitrate and urea, as neither step is found in the decomposition of either pure urea or pure nitrate. This indicates there are reactions between the product of urea decomposition and the remaining solid of the nitrate decomposition. During these steps, the products of urea decomposition reduce NiO to metallic nickel, create CO_2, other volatile oxides, create a graphite layer, and generate some polymeric substance.

Support for the suggestion that the white film found downstream on the cool parts of the reactor is a by-product of the urea decomposition: It was found for both the mixture of urea and nitrate and urea-only controls. XRD analysis of scrapping from the film shows a peak consistent with the urea reflection, and two peaks, close to 20 and 30° 2θ, of very low intensities that were not identified. The latter are thought to be consistent with higher molecular weight by-products, capable of polymerization,

https://doi.org/10.1557/jmr.2010.66 Published online by Cambridge University Press

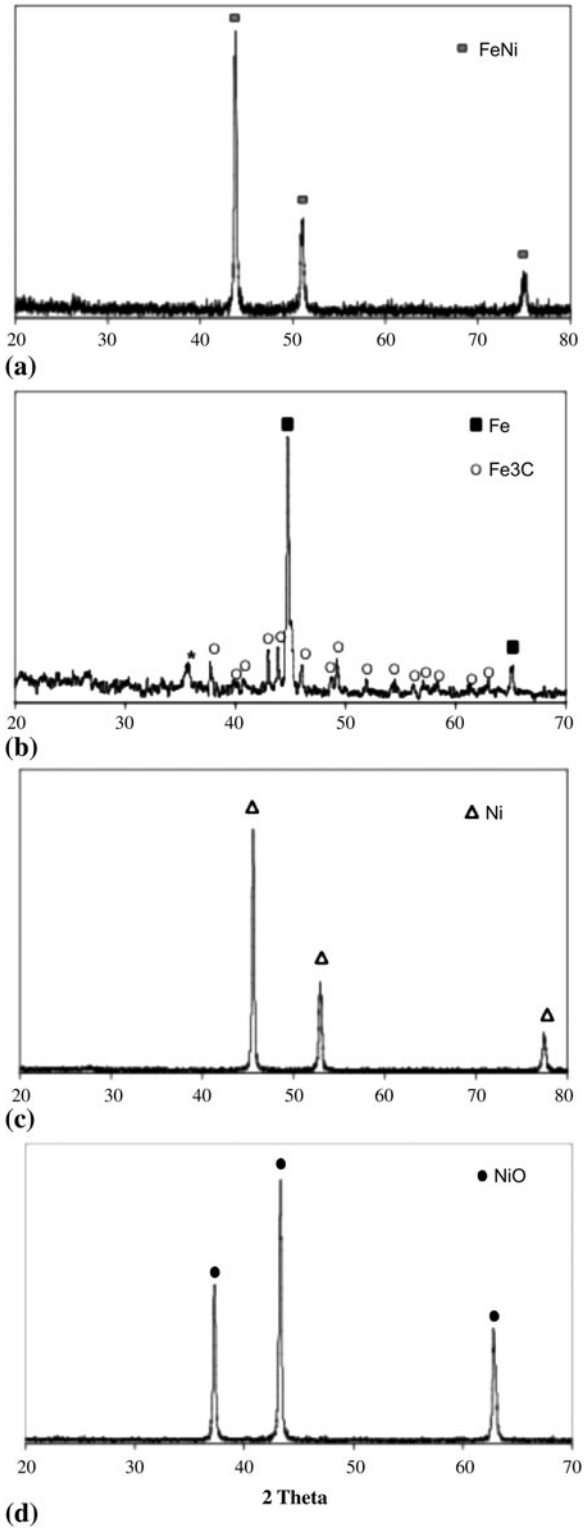


FIG. 4. Metal in XRD. (a) XRD clearly shows that the only metal phase present is FeNi alloy. There is possible evidence of graphite at ~26° 2θ. The peaks are in the intensity ratio reported for randomly oriented samples. (b) In the case of iron nitrate, both metallic iron and iron carbide (Fe_3C) are present. (c) Only metallic nickel is generated from a urea/Ni nitrate mix, although the hint of a peak at $2\theta = 26°$ suggests some graphite is present. (d) In contrast, in the absence of urea only NiO forms.

formed during the thermal decomposition of urea.[36] Alternatively, more complex chemistry could be producing higher molecular weight by-products due to the convolution of the various decomposition processes.

The TGA data (Figure 7) can also be used to determine both the weight of carbon and the fraction of carbon from urea remaining in solid form. First, assuming the only solid products are pure metal and carbon indicates that the final product is 1.2% C by weight. Moreover, assuming all the metal remains in the solid form, only about 0.3% of the carbon initial present in the mixture remains. That is, more than 99% of the carbon atoms in the original urea form some type of volatile species.

IV. DISCUSSION

A. Phenomenon

This is the first study of the reductive/expansion technique for the generation of metallic nanoparticles, and micrometer-scale agglomerates, from molecular precursors. The results clearly indicate that both metal and metal alloy particles can be created simply by rapidly heating, in an inert atmosphere, a physical mix of (i) urea and (ii) nitrates of either iron, nickel, or a combination of both, to a temperature sufficient to ensure complete decomposition (~500 °C). Using particular mixes and protocols FeNi, Fe (some carbide), and Ni particles, all with primary particle sizes less than 200 nm on average were produced. Studies to test the impact of changing the mixing procedure, heating rates, nitrate/urea ratios, and other parameters on average particle size, the character of the particle size distribution, are justified. One question: Is it possible to create very small (~10 nm) metallic and alloy nanoparticles using this approach?

B. Mechanism

The mechanism is less clear than the phenomenon, but nonetheless the data suggest a scheme. Indeed, it is likely the process occurs in three, partially overlapped, stages. First, the nitrates decompose to create oxide particles. This step is very similar to "combustion synthesis," as discussed below. Second, but somewhat overlapping in time/temperature, the urea decomposes, creating reducing species. Finally, the reducing species react with and reduce the metal oxide particles, creating additional volatiles in the process. Moreover, the rapid generation of gases appears to "blow apart" most oxide aggregates, leaving an easily spread paste of primary metal particles in the size range of 50 to 250 nm and some (apparently) weakly bonded agglomerates.

The most important data in support of this postulated mechanism is the similarity of primary particle size in the mixture (metal) and "neat" nitrate (metal oxide) cases.

https://doi.org/10.1557/jmr.2010.66 Published online by Cambridge University Press

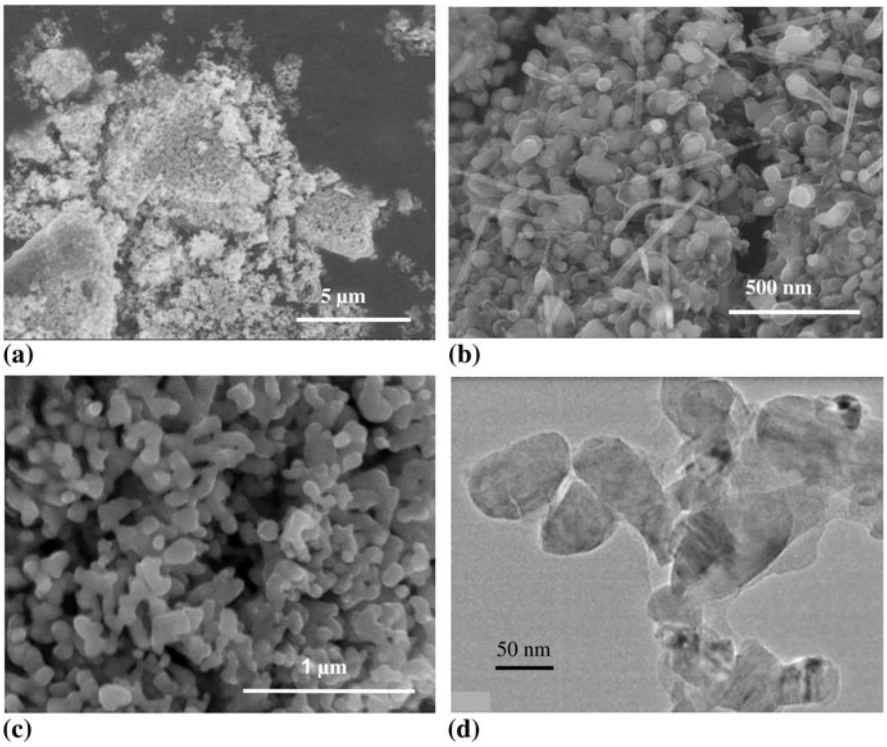


FIG. 5. SEM and TEM of Fe only. (a) Low-magnification SEM (upper left) shows that micron-scale particles are agglomerates of nanoscale primary particles. (b) and (c) Higher-magnification SEM indicates the primary particles are no more than about 150 nm in maximum dimension. Also, in (b) it is evident that there are fibers. There are no "fibers" in (c) and in fact, fibers are found in roughly 50% of the sample. EDS analysis suggests the fibers are iron carbide (see Fig. 4, bottom). (d) TEM data is consistent with SEM data.

This suggests that the nitrates decompose to form oxide particles, as reported elsewhere,[30–32] but in the presence of urea they are subsequently reduced without a dramatic change in the size of the primary particles. Earlier reports have no microscopy and report primarily XRD. The XRD is consistent with that reported here: Oxides are produced in all cases. In particular, physical mixtures of iron and nickel nitrate upon decomposition will produce mixed-cation ($NiFe_2O_4$) oxide. This earlier result is consistent with the finding that mixed nitrates/urea will produce alloy metal particles. Step 1 is the production of mixed cation oxides, and subsequent steps reduce these particles to alloys. No modification is required to the mechanism postulated herein to explain alloy formation.

It is also notable that the submicron primary oxide particles are nearly all bound in large aggregates (approximately >10 μm). In contrast, most of the metal particles are found in small agglomerates (<1 μm), and our qualitative experience is that these agglomerates are weakly bound, easily "smeared" simply with a "light touch" from a small spatula.

Other metal nanoparticles can probably be generated in this fashion, but it is clear from preliminary work with aluminum that the method, at least for the synthesis of nanoparticles, is limited to treatment temperatures below that of the melting temperature of the target metal.

C. Background

Two questions regarding this process are discussed in detail below in the context of earlier literature. First, is the production of reduced species anticipated? Second, is the process described herein truly unique?

The answer to the first question is consistent with precedent. Urea [$(NH_2)_2CO$] and ammonia (NH_3) have been know to reduce nitrogen oxide (NOx) by-products since the 1970s and are extensively used in hydrocarbon-powered electric-generating plants to convert pollutant NOx into N_2 and CO_2 and water.[37–43] Recent research efforts present alternatives to SCR applied to diesel exhausts that might allow the use of different catalyst or temperature modification to the urea thermolysis.[44–46] In other words, SCR and other studies show that the thermal decomposition of urea creates species, probably CO, H_x, and NH_x groups, that are very active for reduction. In the SCR, this results in the reduction of NO_x groups, whereas in the RES process described herein, this results in the reduction of metal oxides, produced "concomitantly" by the decomposition of metal nitrates, to form metal.

Is this technique truly unique? The present work may easily be incorrectly conflated with combustion synthesis (CS).[47] To generate powders, including nanopowders, it is generally understood that CS is a two-step process.[48] First,

https://doi.org/10.1557/jmr.2010.66 Published online by Cambridge University Press

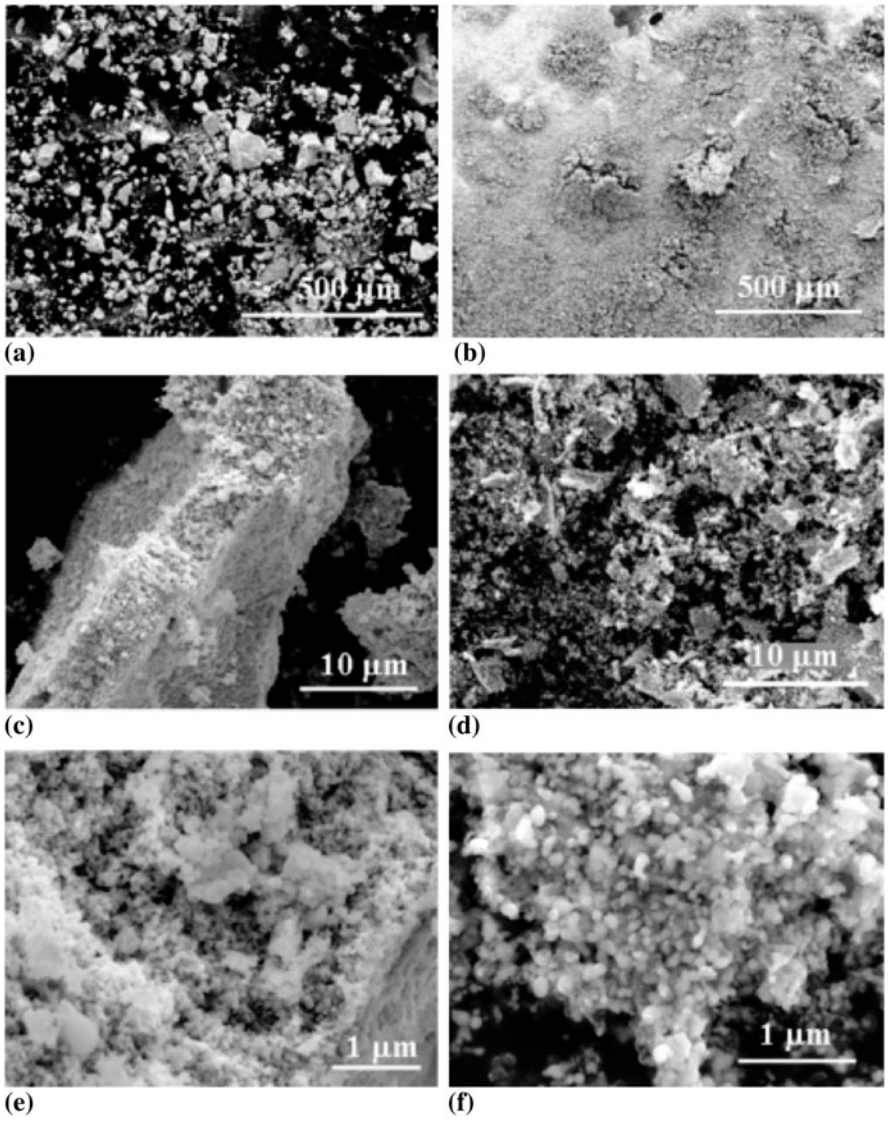


FIG. 6. SEM Ni nitrate/urea contrasted with Ni nitrate only. On the left [(a), (c), (e)] are three different magnifications of particles made by heating Ni nitrate only, after light spreading with a small spatula. The large particles (approximately >10 m) are clearly aggregates of submicron scale NiO particles. On the right [(b), (d), (f)] are particles made by heating physical mixtures of urea and Ni nitrate, after light spreading with a small spatula. The small agglomerates (<2 m) are composed of submicron scale metal particles.

at relatively low temperatures (~200 °C) there is a rapid "ignition" involving only fuel and oxidizer in the material. This is followed by a slower combustion involving oxygen from the air. It is believed the process requires that the heat released by combustion to propel/maintain a combustion front through a precursor powder bed to create oxides and occasionally other ionically bonded structures (e.g., chlorides). At the combustion front, exothermic processes take place that generate heat, promulgating the decomposition process in the next "layer," etc. Although it is argued that the two processes (CS and RES) are initially the same, the final chemistry and outcome are dramatically different. RES creates zero valent metals; from ionically bonded precursors, CS, generates oxides or other ionic structures.

To make the case that the present work is not a variety of combustion synthesis, a review of the entire field is not needed. It is appropriate simply to contrast the use of nitrate precursors in combustion synthesis with that of synthesis from nitrates employing the RES approach. For example in all recent CS studies of synthesis from nitrates, temperatures (~300 °C) far lower than those used here (~800 °C) were used to "ignite" the combustion process required for oxide synthesis. Jovic et al.[49] made Sb_2CoO_6 from a mixture of Sb metal and Co $(NO_3)_2{\cdot}6H_2O$. These materials were mixed with acids, then dried at 80 °C. The dry gel thus formed was heated in air, and, not surprisingly, a mixed metal oxide powder was produced. Garcia et al.[50] created various mixed metal oxides of In–Ga using combustion synthesis starting from

https://doi.org/10.1557/jmr.2010.66 Published online by Cambridge University Press

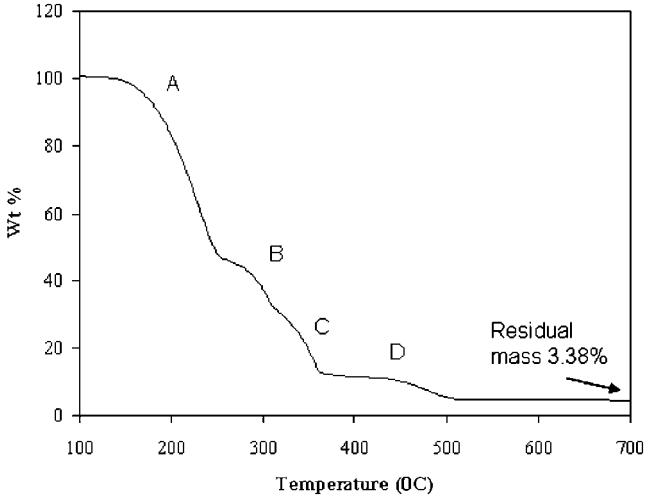


FIG. 7. TGA study. Combination of urea and nickel nitrate showing a residual mass of 3.38% of the initial weight and step stages in the urea and nitrate decomposition.

$In(NO_3)_3{\cdot}H_2O$, $Ga(NO_3)_3{\cdot}6H_2O$ mixed with hydrazine under argon. In that study, in earlier studies of "neat" nitrate decomposition,[30–32,51,52] and in the present study (pure nitrate "controls"), nitrates decompose to oxides upon heating. No oxygen gas necessary.

In fact, there are a host of recent articles on the use of combustion synthesis, employing nitrates, which generate nanoparticle oxides.[53–57] Clearly, combustion synthesis, employing metal nitrates, to make nano-oxide particles is a widely used, well-established, synthesis technique for making metal oxide particles. Moreover, it is postulated that "combustion synthesis" is the first step in the three-step RES process. That is, the decomposition of nitrates to form oxide particles is the same process in both CS and RES. The remaining steps, because of the presence of urea, are not at all related to CS.

Other sets of processes with similar names, field-assisted combustion synthesis (FACS) and pressure-assisted FACS, are dramatically different than standard combustion synthesis in terms of both process and outcome, suggesting FACS is fundamentally different than combustion synthesis,[58–60] and, unlike CS, shares no mechanistic steps with RES. First, in terms of process, in all cases high currents and/or voltages are used. Second, these processes generally occur over time frames of hours. Next, reduced species are produced in environments in which gas-phase oxygen has been excluded. In no case are metals generated.

V. SUMMARY

The most notable result of the present work is the clear demonstration of a novel means to produce submicron and nanometal particles and alloys simply by heating a physical mixture of urea and metal nitrates to a temperature greater than the decomposition temperature of urea. Given that submicron and nanometal particles were produced very rapidly with very simple/standard equipment, it appears the process can be readily scaled. One caveat to this first study: All the particles are coated in a thin layer (approximately <20 Å) of graphite. A thin layer of carbon also presents possibilities, such as a means to create hollow graphitic shells.[61] Alternatively, graphite-coated metals may have value in next-generation batteries and other devices. The ability of this process to create many metals (those that do not readily form carbides) may make this a valuable technique for some applications.[62]

A simple model is consistent with all observation: Upon heating there are two decomposition processes that are convoluted. Initially, the nitrates decompose forming submicron oxides. (Note: This step is very much the same as many "combustion synthesis" processes.) Subsequently, gas species created by the decomposition of urea, chemically reduce the oxide particles formed in the first step. Moreover, the rapid generation of gases attributed to urea decomposition is believed to "shatter" any large aggregates, leaving only small, easily spread, metallic particle agglomerates.

The details of the chemistry of the convoluted decomposition processes are clearly complex. For example, the decomposition of the urea produces both reducing gases, and some volatile carbon, probably in the form of radicals.[63,64] The former leads to the reduction of metal oxides and the latter to the creation of a thin layer of graphitic carbon.

The RES process synthesis is apparently inherently scalable, and as the process is rapid and localized, it is reasonable to imagine a continuous processing variation. However, it is clear that further studies are required to determine if RES yields submicron and/or nanoparticles with lower energy, capital, and time costs than other methods for making nanometal particles.

REFERENCES

1. W.J.M. Mulder, G.J. Strijkers, G.A.F. vanTilborg, A.W. Griffioen, and K. Nicolay: Lipid-based nanoparticles for contrast-enhanced MRI and molecular imaging. *NMR Biomed.* **19**, 142 (2006).
2. M.E. McHenry, S.A. Majetich, and E.M. Kirkpatrick: Synthesis, structure, properties and magnetic applications of carbon-coated nanocrystals produced by a carbon arc. *Mater. Sci. Eng. A* **204**, 19 (1995).
3. J.W.M. Bulte and M.M.J. Modo: *Nanoparticles in Biomedical Imaging: Emerging Technologies and Applications* (Springer-Verlag, New York, 2008).
4. J. Phillips: Plasma generation of supported metal catalysts. U.S. Patent No. 5,989,648 (1999).
5. J. Phillips, S. Shim, I.M. Fonseca, and S. Carabineiro: Plasma generation of supported metal catalysts. *Appl. Catal.* **237**, 41 (2002).
6. H. Zea, C-K. Chen, K. Lester, A. Phillips, A. Datye, I. Fonseca, and J. Phillips: Plasma torch generation of carbon supported metal catalysts. *Catal. Today* **89**, 237 (2004).

https://doi.org/10.1557/jmr.2010.66 Published online by Cambridge University Press

7. J. Phillips, L. Cheng, C. Luhrs, H. Zea, M. Courtney, and C. Hanson: Plasma torch production of Ti–Al nanoparticles, in *Nanophase and Nanocomposite Materials V*, edited by S. Komarneni, K. Kaneko, J.C. Parker, and P. O'Brien (Mater. Res. Soc. Symp. Proc. **1056E**, Warrendale, PA, 2008), HH08–42.
8. J. Phillips, C. Luhrs, and P. Fanson: Production of complex cerium–aluminum oxides using an atmospheric pressure plasma torch. *Langmuir* **23**, 7055 (2007).
9. J. Phillips, C. Luhrs, C. Peng, and P. Fanson: Engineering aerosol through-plasma torch ceramic particulate structures: Influence of precursor composition. *J. Mater. Res.* **23**, 1870 (2008).
10. J. Phillips, C.C. Luhrs, and M. Richard: Engineering particles using the aerosol-through-plasma method. *IEEE Transactions on Plasmas* **37**, 726 (2009).
11. G.L. Messing, S.C. Zhang, and G.V. Jayanthi: Ceramic powder synthesis by spray pyrolysis. *J. Am. Ceram. Soc.* **76**, 2707 (1993).
12. A. Gurav, T. Kodas, T. Pluym, and Y. Xiong: Aerosol processing of materials. *Aerosol Sci. Technol.* **19**, 411 (1993).
13. R. Mueller, R. Jossen, S.E. Pratsinis, M. Watson, and M.K. Akhtar: Zirconia nanoparticles made in spray flames at high production rates. *J. Am. Ceram. Soc.* **87**, 197 (2004).
14. R. Strobel and S.E. Pratsinis: Flame aerosol synthesis of smart nanostructured materials. *J. Mater. Chem.* **17**, 4743 (2007).
15. R.N. Grass and W. Stark: Gas phase synthesis of fcc-cobalt nanoparticles. *J. Mater. Chem.* **16**, 1825 (2006).
16. W. Gong, H. Li, Z.G. Zhao, and J.C. Chen: Ultrafine particles of Fe, Co, and Ni ferromagnetic metals. *J. Appl. Phys.* **69**, 5119 (1991).
17. S. Panda and S.E. Pratsinis: Modeling the synthesis of aluminum particles by evaporation–condensation in an aerosol flow reactor. *Nanostruct. Mater.* **5**, 755 (1995).
18. H.J. Fecht: Synthesis and properties of nanocrystalline metals and alloys prepared by mechanical attrition. *Nanostruct. Mater.* **1**, 125 (1992).
19. V. Haas and R. Birringer: The morphology and size of nanostructured Cu, Pd and W generated by sputtering. *Nanostruct. Mater.* **1**, 491 (1992).
20. J.A. Eastman, L.J. Thompson, and D.J. Marshall: Synthesis of nanophase materials by electron beam evaporation. *Nanostruct. Mater.* **2**, 377 (1993).
21. P.J. Herley and W. Jones: Nanoparticle generation by electron beam induced atomization of binary metal azides. *Nanostruct. Mater.* **2**, 553 (1993).
22. K. Recknagle, Q. Xia, J.N. Chung, C.T. Crowe, H. Hamilton, and G.S. Collins: Properties of nanocrystalline zinc produced by gas condensation. *Nanostruct. Mater.* **4**, 103 (1994).
23. J.P. Chen, C.M. Sorensen, K.J. Klabunde, G.C. Hadjipanayis, E. Devlin, and A. Kostikas: Enhanced magnetization of nanoscale colloidal cobalt particles. *Phys. Rev. B, Condens. Matter* **51**(11), 527 (1995).
24. T. Yamamoto and J. Mazumder: Synthesis of nanocrystalline $NbAl_3$ by laser ablation technique. *Nanostruct. Mater.* **7**, 305 (1996).
25. T. Majima, T. Miyahara, K. Haneda, T. Ishii, and M. Takami: Preparation of iron ultrafine particles by the dielectric breakdown of $Fe(CO)_5$ using a transversely excited atmospheric CO_2 laser and their characteristics. *Jpn. J. Appl. Phys.* **33**, 4759 (1994).
26. Y. Sawada, Y. Kageyama, M. Iwata, and A. Tasaki: Synthesis and magnetic properties of ultrafine iron particles prepared by pyrolysis of carbonyl iron. *Jpn. J. Appl. Phys.* **31**, 3858 (1992).
27. M. AlHaik, C. Hanson, C. Luhrs, M. Tehrani, J. Phillips, and S. Miltenberger: Synthesis and characterisation of nano alumina dental filler. *Int. J. Nano and Biomaterials* **1**, 411 (2008).
28. C.C. Luhrs, J. Phillips, and P. Fanson: Production of unique structures using the aerosol through plasma process. *WIT Trans. Built Environ.* **97**, 63 (2008).
29. C.C. Luhrs, L. Cheng, J. Phillips, and P. Fanson: Plasma generation of nanoparticles for high temperature composite applications. *Int. J. Mater. Struct. Integrity*. **2/3**, 247 (2009).
30. W. Brockner, C. Ehrhardt, and M. Gjikaj: Thermal decomposition of nickel nitrate hexahydrate, $Ni(NO_3)_2\ 6H_2O$ in comparison with $Co(NO_3)_2\ 6H_2O$ and $Ca(NO_3)_2\ 4H_2O$. *Thermochim. Acta* **456**, 64 (2007).
31. M.A.A. Elmasry, A. Gaber, and E.M.H. Khater: Thermal decomposition of Ni(II) and Fe(III) nitrates and their mixtures. *J. Therm. Anal.* **52**, 489 (1998).
32. L.J.E. Hofer, E.M. Cohn, and W.C. Peebles: Isothermal decomposition of nickel carbide. *J. Phys. Chem.* **54**, 1161 (1950).
33. A. Teleki, R. Wengeler, L. Wengeler, H. Nirschi, and S.E. Pratsinix: Distinguishing between aggregates and agglomerates of fame-made TiO_2 by high-pressure dispersion. *Powder Technol.* **181**, 292 (2008).
34. P.A. Schaber, J. Colson, S. Higgins, D. Thielen, B. Anspach, and J. Brauer: Thermal decomposition (pyrolysis) of urea in an open reaction vessel. *Thermochim. Acta* **424**, 131 (2004).
35. N.N. Kostyuk: Thermolysis of urea complexes of uranyl nitrate. *Radiochemistry* **47**, 153 (2004).
36. M. Koebel and M. Elsener: Determination of urea and its thermal decomposition products by high-performance liquid chromatography. *J. Chrom. A* **689**, 164 (1995).
37. H.L. Fang and H.F.M. DaCosta: Urea thermolysis and NOx reduction with and without SCR catalyst. *Appl. Catal. B* **46**, 17 (2003).
38. F. Nakajima and I. Hamada: The state-of-the-art technology of NOx control. *Catal. Today* **29**, 109 (1996).
39. J.R. Gladden: Ammonia/fuel ratio control system for reducing nitrogen oxide emissions. U.S. Patent No. 4,403,473 (1981).
40. W.R. Epperly, J.D. Peter-Hoblyn, G.F. Shulof, Jr., J.C. Sullivan, B.N. Sprague, and J.H. O'Leary: Multi-stage process for reducing the concentration of pollutants in an effluent. U.S. Patent No. 5,057,293 (1991).
41. B.K. Luftglass, W.H. Sun, and J.E. Hofmann: Catalytic/non-catalytic combination process for nitrogen oxides reduction. U.S. Patent No. 5,139,754 (1992).
42. W.H. Sun, J.E. Hofmann, and M.L. Lin: Highly efficient hybrid process for nitrogen oxides reduction. U.S. Patent No. 5,286,467 (1994).
43. F.X. Gibbons, A.L. Huhmann, and A.J. Wallace: Hybrid SCR/SNCR process. U.S. Patent No. 5,853,683 (1998).
44. M. Koebel, M. Elsener, and M. Klemann: Urea-SCR: A promising technique to reduce NOx emissions from automotive diesel engines. *Catal. Today* **59**(3–4), 335 (2000).
45. M. Koebel, M. Elsener, and G. Madia: Reaction pathways in the selective catalytic reduction process with NO and NO_2 at low temperatures. *Ind. Eng. Chem. Res.* **40**(1), 52 (2001).
46. T.J. Wang, S.W. Baek, S.Y. Lee, D.H. Kang, and G.K. Yeo: Experimental investigation on evaporation of urea-water solution droplet for SCR applications. *AlCHE J*. **55**(12), 3267 (2009).
47. A. Varma and J.P. Lebrat: Combustion synthesis of advanced materials. *Chem. Eng. Sci.* **47**, 2179 (1992).
48. K. Deshpande, A. Mukasyan, and A. Varma: Direct synthesis of iron oxide nanopowders by the combustion approach: Reaction mechanism and properties. *Chem. Mater.* **16**, 4896 (2004).
49. M. Jovic, M. Dasic, K. Holl, D. Ilic, and S. Mentus: Gel-combustion synthesis of $CoSb_2O_6$ and its reduction to powdery Sb_2Co alloy. *J. Serb. Chem. Soc.* **74**, 53 (2009).
50. R. Garcia, G.A. Hirata, and J. McKittrick: New combustion synthesis technique for the production of $(In_xGa_{1-x})_2O_3$ powders: Hydrazine/metal nitrate method. *J. Mater. Res.* **16**, 1059 (2001).
51. A. Dutta, S. Patra, V. Bedekar, A.K. Tyagi, and R.N. Basu: Nanocrystalline gadolinium doped ceria: Combustion synthesis and electrical characterization. *J. Nanosci. Nanotechnol.* **9**, 3075 (2009).

https://doi.org/10.1557/jmr.2010.66 Published online by Cambridge University Press

52. B. Mandal, A. Dutta, S.K. Deshpande, R.N. Basu, and A.K. Tyagi: Nanocrystalline $Nd_{2-y}Gd_yZr_2O_7$ pyrochlore: Facile synthesis and electrical characterization. *J. Mater. Res.* **24**, 2855 (2009).
53. B. Jurca, C. Paraschi, A. Ianculescu, and O. Carp: Thermal behaviour of the system $Fe(NO_3)_3{\cdot}9H_2O$–$Bi_5O(OH)_9(NO_3)_4{\cdot}9H_2O$–glycine/urea and of their generated oxides ($BiFeO_3$). *J. Therm. Anal. Calorim.* **97**, 91 (2009).
54. R. Ianos, I. Lazau, and C. Pacurariu: Metal nitrate/fuel mixture reactivity and its influence on the solution combustion synthesis of γ-$LiAlO_2$. *J. Therm. Anal. Calorim.* **97**, 209 (2009).
55. R.V. Mangalaraja, S. Ananthakumar, J. Mouzon, K. Uma, M. Lopez, C.P. Camurri, and M. Oden: Synthesis of nanocrystalline yttria through in-situ sulphated-combustion technique. *J. Ceram. Soc. Jpn.* **117**, 1065 (2009).
56. K.S. Martirosyan, L. Wang, A. Vicent, and D. Luss: Synthesis and performance of bismuth trioxide nanoparticles for high energy gas generator use. *Nanotechnology* **20**, 405609 (2009).
57. V.R.S. Ningthoujam, R. Shukla, R.K. Vatsa, V. Duppel, L. Kienle, and A.K. Tyagi: Gd_2O_3:Eu^{3+} particles prepared by glycine-nitrate combustion: Phase, concentration, annealing, and luminescence studies. *J. Appl. Phys.* **105**, 084304 (2009).
58. Z.A.R. Munir, W. Lai, and K.H. Ewald: Field assisted combustion synthesis. U.S. Patent No. 5,380,409 (1995).
59. A. Feng, T. Orling, and Z.A.R. Munir: Field activated pressure assisted combustion synthesis of polycrystalline Ti_3SiC_2. *J. Mater. Res.* **14**, 925 (1999).
60. G. Jiang, H. Zhuang, and W. Li: Combustion synthesis of tungsten carbides under electric field II: Field activated pressure assisted combustion synthesis. *Ceram. Int.* **30**, 191 (2004).
61. J. Phillips, T. Shiina, M. Nemer, and K. Lester: Graphitic structures by design. *Langmuir* **22**, 9694 (2006).
62. C. Luhrs, J. Phillips, M. Richard, and K. Stamm: Material with core-shell structure-2. U.S. Patent Application 20,090,317,719 (2009).
63. M.A. Atwater, J. Phillips, and Z.C. Leseman: Formation of carbon nanofibers and thin films catalyzed by palladium in ethylene-hydrogen mixtures. *J. Phys. Chem.* **114**, 5804 (2010).
64. M.A. Atwater, J. Phillips, S.K. Doorn, C.C. Luhrs, Y.F. Diez, J.A. Menendez, and Z.C. Leseman: Palladium catalyzed growth of carbon nanofibers and thin films in a partial combustion environment. *Carbon* **47**, 2269 (2009).

https://doi.org/10.1557/jmr.2010.66 Published online by Cambridge University Press